Steel and Composite Structures, Vol. 9, No. 1 (2009) 59-75
DOI: http://dx.doi.org/10.12989/scs.2009.9.1.059

Discrete singular convolution method for bending analysis of Reissner/Mindlin plates using geometric transformation

Ömer Civalek*

Akdeniz University, Faculty of Engineering, Civil Engineering Department, Division of Mechanics, Antalya, Turkey

Engin Emsen

Akdeniz University, Faculty of Engineering Civil Engineering Department, Division of Structures, Antalya, Turkey

(Received January 11, 2008, Accepted January 16, 2009)

Abstract. In this study, a simple approach for bending analysis of Reissner-Mindlin plates is presented using the four-node quadrilateral domain transformation based on discrete singular convolution. In the proposed approach, irregular physical domain is transformed into a rectangular domain by using the geometric coordinate transformation. The DSC procedures are then applied to discrete the governing equations and boundary conditions. The accuracy of the proposed method is verified by comparison with known solutions obtained by other numerical or analytical methods. Results for Reissner-Mindlin plates show a satisfactory agreement with the analytical and numerical solutions.

Keywords : Reissner-Mindlin plate; geometric transformation; plate; bending; discrete singular convolution.

1. Introduction

Plates are widely used in civil, mechanical and aero-space engineering. A variety of theories are available today for static and dynamic analysis of plates. Generally, there are four theories, which are Kirchhoff (thin), Reissner, Mindlin and third-order shear deformation theory of Reddy's. These theories (Reissner 1945, Mindlin 1951, Kirchhoff 1850) have been used extensively for plates. The analysis of non-rectangular plates has been the subject of the research of structural and mechanical engineering. Li *et al*. (1986) presented a spline finite strip analysis of arbitrary shaped general plates. Cheung *et al*. (1988) also developed a finite strip analysis for static and vibration analysis of general plates. For Mindlin-Reissner plate a quadrilateral element proposed by Wanji and Cheung (2000). An improved four-node hybrid-mixed element (Ayad and Rigolot 2002) and a heterosis element (Butalia *et al*. 1990) have been development for skew and rhombic plates based on Mindlin-Reissner plate theory. Following, Liew and Han (1995) and Han and Liew (1997) introduced a mapping technique to apply the differential quadrature (DQ) method for analysis of plates in conjunction with the Reissner-Mindlin thick plate theory. Stability and vibration analyses of thick plates are widely studied by researchers (Liew *et al.*

* Corresponding Author, Email: civalek@yahoo.com

1994, Liew *et al.* 1996, Civalek 2004, Xiang and Wei 2004, Wang *et al*. 1993). DQ solution for shear deformable plates have also been presented by Liew and Liu (2000) and Liu and Liew (1999). Analytical and numerical methods had been used for Mindlin plates having different boundary conditions (Liew and Han 1997, Xian and Zhang 2005, Liu and Liew 1998, Xiang 2003). The primary objective of this study is to explore the application of the DSC method to the bending analysis of Reissner-Mindlin plates. To the author's knowledge, this is the first instance in which the DSC method has been adopted for static analysis of Reissner-Mindlin plates with straight-sided quadrilateral domain.

2. Discrete singular convolution (DSC)

In this section, the method of discrete singular convolution is briefly presented. Details of the DSC method are not given; interested readers may refer to the works of (Wei 2001, Wei 2001a, Zhao *et al*. 2002). The method of discrete singular convolutions (DSC) has emerged as a new approach for numerical solutions of differential equations (Wei 2001b, Zhao *et al*. 2002a, Civalek 2006a, Civalek 2007). This new method has a potential approach for computer realization as a wavelet collocation scheme (Wei 2000). The method of DSC is a relatively new numerical technique for approximation of derivatives. The method of discrete singular convolution (DSC) has been increasingly applied to solve differential equations in many engineering and sciences problems (Wei *et al*. 2002, Civalek 2006, Civalek 2007a, Civalek 2007b). In a general definition, numerical solutions of differential equations are formulated by some singular kernels. For brevity, consider a distribution, T and $\eta(t)$ as an element of the space of the test function. A singular convolution can be defined, in the context of distribution theory, by (Wei 2001)

$$F(t) = (T * \eta)(t) = \int_{-\infty}^{\infty} T(t-x)\,\eta(x)dx \tag{1}$$

where $T(t-x)$ is a singular kernel. The DSC algorithm can be realized by using many approximation kernels. However, it was shown that for many problems, the use of the regularized Shannon kernel (RSK) is very efficient. The RSK is given by (Wei 2001a)

$$\delta_{\Delta,\,\sigma}(x-x_k) = \frac{\sin[(\pi/\Delta)(x-x_k)]}{(\pi/\Delta)(x-x_k)}\exp\left[-\frac{(x-x_k)^2}{2\sigma^2}\right];\sigma>0 \tag{2}$$

where $\Delta = \pi/(N-1)$ is the grid spacing and N is the number of grid points. The parameter σ determines the width of the Gaussian envelope and often varies in association with the grid spacing, i.e., $\sigma = r$h. In the DSC method, the function $f(x)$ and its derivatives with respect to the x coordinate at a grid point x_i are approximated by a linear sum of discrete values $f(x_k)$ in a narrow bandwidth $[x - x_M, x + x_M]$. For numerical computations, this can be expressed as (Wei *et al*. 2002)

$$\left.\frac{d^n f(x)}{dx^n}\right|_{x=x_i} = f^{(n)}(x) \approx \sum_{k=-M}^{M} \delta^{(n)}_{\Delta,\sigma}(x_i - x_k) f(x_k);\ (n = 0, 1, 2, \ldots,) \tag{3}$$

where superscript n denotes the nth-order derivative with respect to x. The x_k is a set of discrete sampling points centred around the point x, σ is a regularization parameter, Δ is the grid spacing, and 2M + 1 is the computational bandwidth, which is usually smaller than the size of the computational domain. It is also known that, it provides exact results when sampling points are extended to an infinite series given by

$$f(x) = \sum_{k=-\infty}^{\infty} f(x_k) = \frac{\sin[(\pi/\Delta)(x-x_k)]}{(\pi/\Delta)(x-x_k)} \quad \forall f \in B^2_{\pi/\Delta} \tag{4}$$

The discretized forms of Eq. (3) can then be expressed as

$$f^{(n)}(x) = \left.\frac{d^n f}{dx^n}\right|_{x=x_i} \approx \sum_{k=-M}^{M} \delta^{(n)}_{\Delta,\sigma}(k\Delta x_N) f_{i+k,j}\,. \tag{5}$$

When the regularized Shannon's delta (RSD) kernel is used, the detailed expressions for, $\delta^{(n)}_{\Delta,\sigma}(x)$ can be easily obtained. Detailed formulations for these differentiation coefficients can be found in references (Wei 2001).

3. DSC method for irregular domains

Consider an arbitrary straight-sided quadrilateral plate in the Cartesian x-y plane, as shown in Fig. 1. The geometry of this plate can be mapped into a rectangular plate in the natural ξ-η plane.
By employing the following transformation equations the physical domain is mapped into the computational domain

$$x = \sum_{i=1}^{N} \Phi_i(\xi, \eta) x_i) \quad \text{and} \quad y = \sum_{i=1}^{N} \Phi_i(\xi, \eta) y_i \tag{6,7}$$

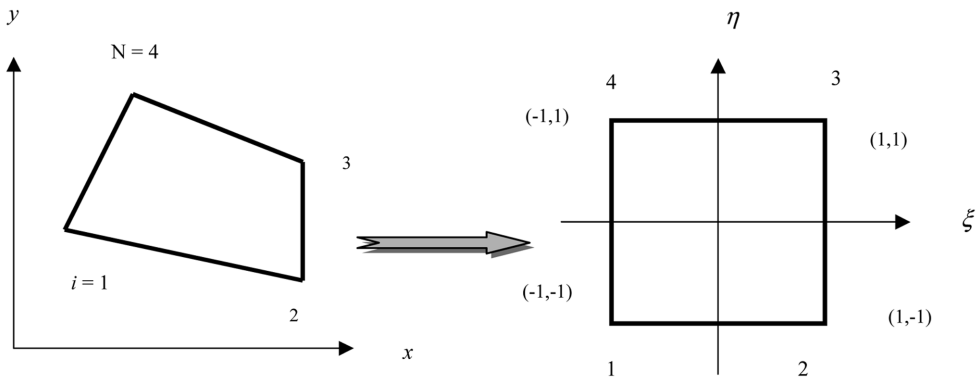

Fig. 1 Mapping of arbitrary quadrilateral plates into natural coordinates

where x_i and y_i are the coordinates of node i in the physical domain, N is the number of grid points, and $\Phi_i(\xi, \eta)$; i= 1,2,3,…,N are the interpolation or shape functions. These are given for node i;

$$\Phi_i(\xi, \eta) = \frac{1}{4}(1 + \xi\xi_i)(1 + \eta\eta_i) \tag{8}$$

Using the chain rule, the first-order, and second order derivatives of a function are given

$$\begin{Bmatrix} u_x \\ u_y \end{Bmatrix} = [J_{11}]^{-1} \begin{Bmatrix} u_\xi \\ u_\eta \end{Bmatrix} \tag{9}$$

$$\begin{Bmatrix} u_{xx} \\ u_{yy} \\ 2u_{xy} \end{Bmatrix} = [J_{22}]^{-1} \begin{Bmatrix} u_{\xi\xi} \\ u_{\eta\eta} \\ 2u_{\xi\eta} \end{Bmatrix} - [J_{22}]^{-1}[J_{21}][J_{11}]^{-1} \begin{Bmatrix} u_\xi \\ u_\eta \end{Bmatrix} \tag{10}$$

where ξ_i and η_i are the coordinates of Node i in the ξ-η plane, and J_{ij} are the elements of the Jacobian matrix. These are expressed as follows;

$$[J_{11}] = \begin{bmatrix} x_\xi & y_\xi \\ x_\eta & y_\eta \end{bmatrix}, \quad [J_{21}] = \begin{bmatrix} x_{\xi\xi} & y_{\xi\xi} \\ x_{\eta\eta} & y_{\eta\eta} \\ x_{\xi\eta} & y_{\xi\eta} \end{bmatrix} \tag{11, 12}$$

$$[J_{22}] = \begin{bmatrix} x_\xi^{\,2} & y_\xi^{\,2} & x_\xi y_\xi \\ x_\eta^{\,2} & y_\eta^{\,2} & x_\eta y_\eta \\ x_\xi x_\eta & y_\xi y_\eta & \frac{1}{2}(x_\xi y_\eta + x_\eta y_\xi) \end{bmatrix}. \tag{13}$$

The above transformations will be used later to transform the governing differential equations and related boundary conditions from the physical domain x-y into the computational domain ξ-η. Thus an arbitrary-shaped quadrilateral plate may be represented by the mapping of a square plate defined in terms of its natural coordinates. The equations of any-order derivatives can be easily written at any point. First-order derivatives, for example, can be given by

$$\frac{\partial(\ )}{\partial x} = [J_{11}]^{-1} \sum_{i=-M}^{M} \delta^{(1)}_{\Delta,\sigma}(k\Delta\xi)(\ )_{ik} \tag{14}$$

Similarly, the second-order derivatives with respect to the -x and y-coordinate can be written

respectively, as

$$\frac{\partial^2(\ )}{\partial x^2} = [J_{22}]^{-1} \sum_{i=-M}^{M} \delta^{(2)}_{\Delta,\sigma}(k\Delta\xi)(\ )_{ik} - [J_{22}]^{-1}[J_{21}][J_{11}]^{-1} \sum_{i=-M}^{M} \delta^{(1)}_{\Delta,\sigma}(k\Delta\xi)(\ )_{ik} \tag{15}$$

$$\frac{\partial^2(\ )}{\partial y^2} = [J_{22}]^{-1} \sum_{i=-M}^{M} \delta^{(2)}_{\Delta,\sigma}(k\Delta\eta)(\ )_{jk} - [J_{22}]^{-1}[J_{21}][J_{11}]^{-1} \sum_{i=-M}^{M} \delta^{(1)}_{\Delta,\sigma}(k\Delta\eta)(\ )_{jk} \tag{16}$$

$$\frac{\partial^2(\ )}{\partial x \partial y} = [J_{22}]^{-1} \sum_{i=-M}^{M} \delta^{(1)}_{\Delta,\sigma}(k\Delta\xi) \sum_{i=-M}^{M} \delta^{(1)}_{\Delta,\sigma}(k\Delta\eta)(\ )_{ij} - [J_{22}]^{-1}[J_{21}][J_{11}]^{-1} \sum_{i=-M}^{M} \delta^{(1)}_{\Delta,\sigma}(k\Delta\eta)(\ )_{jk} \tag{17}$$

4. Fundamental equations

The general governing differential equations of Reissner-Mindlin plates for bending are given as

$$\frac{D}{2}\left[(1-\upsilon)\left(\frac{\partial^2\psi_x}{\partial x^2} + \frac{\partial^2\psi_x}{\partial y^2}\right) + (1+\upsilon)\left(\frac{\partial^2\psi_x}{\partial x^2} + \frac{\partial^2\psi_y}{\partial x \partial y}\right)\right] + \kappa Gh\left(\frac{\partial w}{\partial x} - \psi_x\right) = 0, \tag{18}$$

$$\frac{D}{2}\left[(1-\upsilon)\left(\frac{\partial^2\psi_y}{\partial x^2} + \frac{\partial^2\psi_y}{\partial y^2}\right) + (1+\upsilon)\left(\frac{\partial^2\psi_x}{\partial x \partial y} + \frac{\partial^2\psi_y}{\partial y^2}\right)\right] + \kappa Gh\left(\frac{\partial w}{\partial y} - \psi_y\right) = 0, \tag{19}$$

$$\kappa Gh\left(\frac{\partial^2 w}{\partial x^2} + \frac{\partial^2 w}{\partial y^2}\right) - \kappa Gh\left(\frac{\partial \psi_x}{\partial x} + \frac{\partial \psi_y}{\partial y}\right) + q(x,y) = 0. \tag{20}$$

The bending moments and shear forces are also given by the following formulae

$$M_x = -D\left(\frac{\partial \psi_x}{\partial x} + \upsilon\frac{\partial \psi_y}{\partial y}\right), \quad M_y = -D\left(\upsilon\frac{\partial \psi_x}{\partial x} + \frac{\partial \psi_y}{\partial y}\right), \tag{21, 22}$$

$$M_{xy} = -\frac{1-\upsilon}{2}D\left(\frac{\partial \psi_x}{\partial y} + \frac{\partial \psi_y}{\partial x}\right), \tag{23}$$

$$Q_x = \kappa Gh\left(\frac{\partial w}{\partial x} - \psi_x\right), \quad Q_y = \kappa Gh\left(\frac{\partial w}{\partial y} - \psi_y\right). \tag{24}$$

By using the transformation procedures, the governing differential equations take the following discrete form

$$\frac{D}{2}\{(1-\upsilon)\Big[[J_{22}]^{-1}\sum_{i=-M}^{M}\delta^{(2)}{}_{\Delta,\sigma}(k\Delta\xi)(\psi_x)_{ik}-[J_{22}]^{-1}[J_{21}][J_{11}]^{-1}\sum_{i=-M}^{M}\delta^{(1)}{}_{\Delta,\sigma}(k\Delta\xi)(\psi_x)_{ik}$$
$$+[J_{22}]^{-1}\sum_{i=-M}^{M}\delta^{(2)}{}_{\Delta,\sigma}(k\Delta\eta)(\psi_x)_{jk}-[J_{22}]^{-1}[J_{21}][J_{11}]^{-1}\sum_{i=-M}^{M}\delta^{(1)}{}_{\Delta,\sigma}(k\Delta\eta)(\psi_x)_{jk}\Big]$$
$$+(1+\upsilon)\Big[[J_{22}]^{-1}\sum_{i=-M}^{M}\delta^{(2)}{}_{\Delta,\sigma}(k\Delta\xi)(\psi_x)_{ik}-[J_{22}]^{-1}[J_{21}][J_{11}]^{-1}\sum_{i=-M}^{M}\delta^{(1)}{}_{\Delta,\sigma}(k\Delta\xi)(\psi_x)_{ik}$$
$$+[J_{22}]^{-1}\sum_{i=-M}^{M}\delta^{(1)}{}_{\Delta,\sigma}(k\Delta\xi)\sum_{i=-M}^{M}\delta^{(1)}{}_{\Delta,\sigma}(k\Delta\eta)(\psi_y)_{ij}-[J_{22}]^{-1}[J_{21}][J_{11}]^{-1}\sum_{i=-M}^{M}\delta^{(1)}{}_{\Delta,\sigma}(k\Delta\eta)(\psi_y)_{jk}\Big]$$
$$+\kappa Gh\Big([J_{11}]^{-1}\sum_{i=-M}^{M}\delta^{(1)}{}_{\Delta,\sigma}(k\Delta\xi)(w)_{ik}-(\psi_x)_{ik}\Big)=0, \tag{25}$$

$$\frac{D}{2}\{(1-\upsilon)\Big[[J_{22}]^{-1}\sum_{i=-M}^{M}\delta^{(2)}{}_{\Delta,\sigma}(k\Delta\xi)(\psi_y)_{ik}-[J_{22}]^{-1}[J_{21}][J_{11}]^{-1}\sum_{i=-M}^{M}\delta^{(1)}{}_{\Delta,\sigma}(k\Delta\xi)(\psi_y)_{ik}$$
$$+[J_{22}]^{-1}\sum_{i=-M}^{M}\delta^{(2)}{}_{\Delta,\sigma}(k\Delta\eta)(\psi_y)_{jk}-[J_{22}]^{-1}[J_{21}][J_{11}]^{-1}\sum_{i=-M}^{M}\delta^{(1)}{}_{\Delta,\sigma}(k\Delta\eta)(\psi_y)_{jk}\Big]$$
$$+(1+\upsilon)\Big[[J_{22}]^{-1}\sum_{i=-M}^{M}\delta^{(2)}{}_{\Delta,\sigma}(k\Delta\xi)(\psi_y)_{jk}-[J_{22}]^{-1}[J_{21}][J_{11}]^{-1}\sum_{i=-M}^{M}\delta^{(1)}{}_{\Delta,\sigma}(k\Delta\xi)(\psi_y)_{jk}$$
$$+[J_{22}]^{-1}\sum_{i=-M}^{M}\delta^{(1)}{}_{\Delta,\sigma}(k\Delta\xi)\sum_{i=-M}^{M}\delta^{(1)}{}_{\Delta,\sigma}(k\Delta\eta)(\psi_x)_{ij}-[J_{22}]^{-1}[J_{21}][J_{11}]^{-1}\sum_{i=-M}^{M}\delta^{(1)}{}_{\Delta,\sigma}(k\Delta\eta)(\psi_x)_{jk}\Big]$$
$$+\kappa Gh\Big([J_{11}]^{-1}\sum_{i=-M}^{M}\delta^{(1)}{}_{\Delta,\sigma}(k\Delta\eta)(w)_{jk}-(\psi_y)_{jk}\Big)=0, \tag{26}$$

$$\kappa Gh\Big[[J_{22}]^{-1}\sum_{i=-M}^{M}\delta^{(2)}{}_{\Delta,\sigma}(k\Delta\xi)(w)_{ik}-[J_{22}]^{-1}[J_{21}][J_{11}]^{-1}\sum_{i=-M}^{M}\delta^{(1)}{}_{\Delta,\sigma}(k\Delta\xi)(w)_{ik}$$
$$+[J_{22}]^{-1}\sum_{i=-M}^{M}\delta^{(2)}{}_{\Delta,\sigma}(k\Delta\eta)(w)_{jk}-[J_{22}]^{-1}[J_{21}][J_{11}]^{-1}\sum_{i=-M}^{M}\delta^{(1)}{}_{\Delta,\sigma}(k\Delta\eta)(w)_{jk}\Big]$$
$$-\kappa Gh\Big[[J_{11}]^{-1}\sum_{i=-M}^{M}\delta^{(1)}{}_{\Delta,\sigma}(k\Delta\xi)(\psi_x)_{ik}+[J_{11}]^{-1}\sum_{i=-M}^{M}\delta^{(1)}{}_{\Delta,\sigma}(k\Delta\eta)(\psi_y)_{jk}\Big]=0. \tag{27}$$

Similarly, the force resultants are given in the computational domain as

$$-D\left[[J_{11}]^{-1}\sum_{i=-M}^{M}\delta^{(1)}{}_{\Delta,\sigma}(k\Delta\xi)(\psi_x)_{ik}+\upsilon[J_{11}]^{-1}\sum_{i=-M}^{M}\delta^{(1)}{}_{\Delta,\sigma}(k\Delta\eta)(\psi_y)_{jk}\right]=M_x \tag{28}$$

$$-D\left[\upsilon[J_{11}]^{-1}\sum_{i=-M}^{M}\delta^{(1)}{}_{\Delta,\sigma}(k\Delta\xi)(\psi_x)_{ik}+[J_{11}]^{-1}\sum_{i=-M}^{M}\delta^{(1)}{}_{\Delta,\sigma}(k\Delta\eta)(\psi_y)_{jk}\right]=M_y \tag{29}$$

$$-\frac{1-\upsilon}{2}D\left[[J_{11}]^{-1}\sum_{i=-M}^{M}\delta^{(1)}{}_{\Delta,\sigma}(k\Delta\eta)(\psi_x)_{jk}+[J_{11}]^{-1}\sum_{i=-M}^{M}\delta^{(1)}{}_{\Delta,\sigma}(k\Delta\xi)(\psi_y)_{ik}\right]=M_{xy} \tag{30}$$

$$\kappa Gh\left[[J_{11}]^{-1}\sum_{i=-M}^{M}\delta^{(1)}{}_{\Delta,\sigma}(k\Delta\xi)(w)_{ik}-(\psi_x)_{ij}\right]=Q_x \tag{31}$$

$$\kappa Gh\left[[J_{11}]^{-1}\sum_{i=-M}^{M}\delta^{(1)}{}_{\Delta,\sigma}(k\Delta\eta)(w)_{jk}-(\psi_y)_{ij}\right]=Q_y \tag{32}$$

5. Boundary conditions

Two types of boundary conditions are used. Relations of simply supported and clamped boundary conditions for an arbitrary edge are given as

i) Simply supported (S)

$$w=0,\qquad M_n=0\quad\text{and}\quad\psi_s=0 \tag{33a, 33b, 33c}$$

ii) Clamped supported (C)

$$w=0,\qquad \psi_n=0\quad\text{and}\quad\psi_s=0 \tag{34a, 34b, 34c}$$

The force resultants and the deformations on the edge are given as follows:

$$M_n=-n_x^2D\left(\frac{\partial\psi_x}{\partial x}+\upsilon\frac{\partial\psi_y}{\partial y}\right)-2n_xn_y\frac{1-\upsilon}{2}D\left(\frac{\partial\psi_x}{\partial y}+\upsilon\frac{\partial\psi_y}{\partial x}\right)-n_y^2D\left(\upsilon\frac{\partial\psi_x}{\partial x}+\frac{\partial\psi_y}{\partial y}\right) \tag{35}$$

$$\psi_n=n_x\psi_x+n_y\psi_y, \tag{36}$$

$$\psi_s=n_x\psi_x-n_y\psi_x. \tag{37}$$

5.1. Discretization of boundary conditions

By using the transformation rule and employing the method of DSC, the boundary conditions can be given as below

i) Simply supported (S)

$$w_{ij} = 0 \tag{38a}$$

$$\begin{aligned}
&-n_x^2 D\left[[J_{11}]^{-1}\sum_{i=-M}^{M}\delta^{(1)}{}_{\Delta,\sigma}(k\Delta\xi)(\psi_x)_{ik} + \upsilon[J_{11}]^{-1}\sum_{i=-M}^{M}\delta^{(1)}{}_{\Delta,\sigma}(k\Delta\eta)(\psi_y)_{jk}\right]\\
&-n_x n_y\frac{1-\upsilon}{2}D\left[[J_{11}]^{-1}\sum_{i=-M}^{M}\delta^{(1)}{}_{\Delta,\sigma}(k\Delta\eta)(\psi_x)_{jk} + [J_{11}]^{-1}\sum_{i=-M}^{M}\delta^{(1)}{}_{\Delta,\sigma}(k\Delta\xi)(\psi_y)_{ik}\right]\\
&-n_y^2 D\left[\upsilon[J_{11}]^{-1}\sum_{i=-M}^{M}\delta^{(1)}{}_{\Delta,\sigma}(k\Delta\xi)(\psi_x)_{ik} + [J_{11}]^{-1}\sum_{i=-M}^{M}\delta^{(1)}{}_{\Delta,\sigma}(k\Delta\eta)(\psi_y)_{jk}\right] = 0
\end{aligned} \tag{38b}$$

$$n_x(\psi_x)_{ij} - n_y(\psi_x)_{ij} = 0 \tag{38c}$$

ii) Clamped supported (C)

$$w_{ij} = 0 \tag{39a}$$

$$n_x(\psi_x)_{ij} + n_y(\psi_y)_{ij} = 0 \tag{39b}$$

$$n_x(\psi_x)_{ij} - n_y(\psi_x)_{ij} = 0 \tag{39c}$$

6. Numerical results

In this section, a number of numerical examples are given to demonstrate the accuracy, simplicity and applicability of the present DSC method for Reissner-Mindlin straight sided quadrilateral plate bending problems (Figs. 2 to 3). Free vibration analysis of Mindlin plates by DSC-Ritz method were investigated by Hou *et al*. (2002). The values of deflections and moments have all been expressed as non-dimensional quantities.

In order to test the convergency of numerical solutions by present method, central deflections were calculated for a CCCC square plate. The results are given in Table 1, together with exact results (Timoshenko and Krieger 1959) and numerical solutions calculated by Liu and Liew (1998) by applying differential quadrature method. Table 1 shows the good convergency of the numerical solutions for the displacements calculated by present method for $N = 17$ grid numbers.

Fig. 4 gives the convergence of the central deflection of CCCC skew plate. The normalized displacement $w/w(*)$is presented against the number of grid points for different skew angles in this

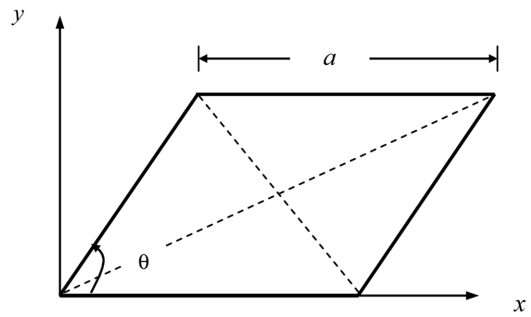

Fig. 2 A typical skew plate

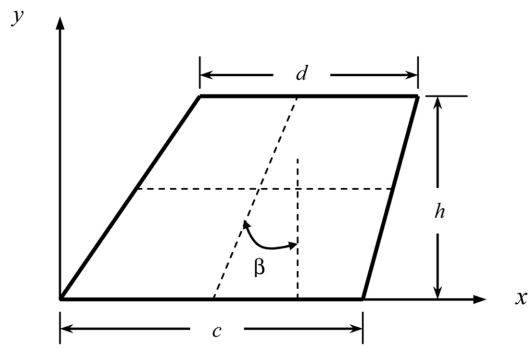

Fig. 3 A trapezoidal plate

figure. The value $w(*)$ is the references solutions taken from Liew and Han (1997). From this figure, it is found that DSC results of skew plate are converging to the reference value with the increase of grid points. Note that the accuracy of the proposed method is suitable when using 15 grid points. A simply supported skew plate is used to check the effect of parameter of DSC kernel r is studied. The results in the form of maximum central deflection under uniformly distributed load. The obtained results are given in Fig. 5 for different grid numbers. The value $w_{max}(*)$ is the references solutions taken from Butalia *et al*. (1990). The effect of thickness h/a, on the convergence is depicted Fig. 6 for skew angle $\theta = 15^o$. It is shown in this figure that the relative thickness ratio is insignificant to convergence rate. Because the reasonable accurate results are obtained for all different relative thickness ratio for N = 15. In other words, with the increase of grid numbers N ($N > 15$), the effect of the h/a on the moments is significant. It is shown that the parameter r is gives more accurate results for the interval $2.4 \le r \le 3.2$ for skew plate. Based on the convergence study given Figs. 4 to 6, unless specified otherwise, we set the grid numbers as $N = 17$. Simply supported (SSSS) square plate and CSCS rectangular plates are solved for uniformly distributed loading. The results are displayed in Table 2 and Table 3. Different aspect ratios and thickness to width ratios are taken into consideration. Table 4 provides the deflections and bending moments of trapezoidal (Fig. 3) plate for the CCCC boundary condition. The following geometric properties are used for the trapezoidal plate: $a/b = 1.0$; $c/a = 0.7$. The central deflection and maximum moment of a skew plate ($h/a = 0.01$) for SSSS and CCCC boundary conditions are given in.

Table 5 presents central deflection with different skew angles (Fig. 2). In Table 6, central deflection

Table 1 Convergence of the deflection $w(qa^4/1000D)$ for a CCCC square plate

h/a	Exact (Timoshenko 1959)	Liu and Liew (1998)	Present DSC Results		
			N = 15	N = 17	N = 21
0.01	-	1.267	1.268	1.266	1.266
0.05	1.325	1.327	1.333	1.327	1.327
0.10	1.496	1.505	1.501	1.498	1.498
0.2	2.135	2.172	2.171	2.166	2.166

and maximum bending moments of a SSSS skew plate are given. Four thickness to width ratio, h/a and five different skew angles are consider. It is also shown that, as the plate thickness is increased, the deflections and moments are found to increase. Maximum deflections of a skew plate under central

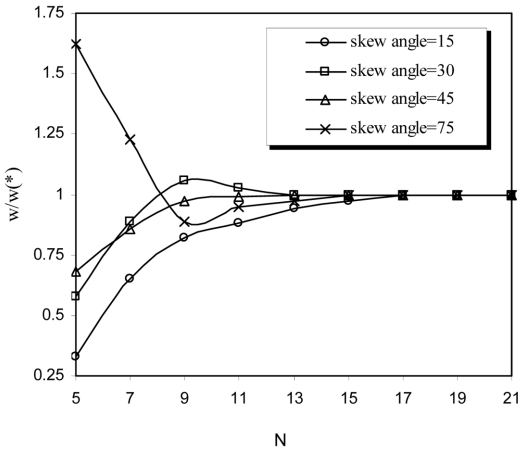

Fig. 4 Convergence of central deflections with grid numbers for different skew angles of CCCC skew plates

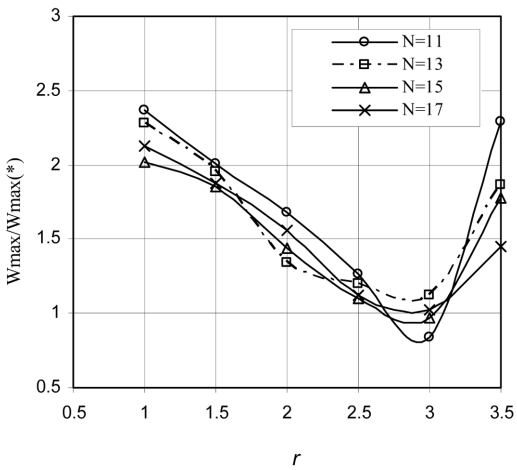

Fig. 5 Convergences of maximum deflections with r of SSSS skew plates for different grid numbers

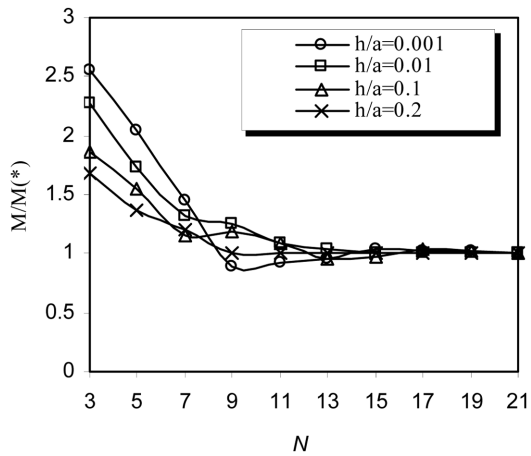

Fig. 6 Convergence of maximum deflections with grid numbers for different thickness of CCCC skew plates

Table 2 Convergence of the bending results for a SSSS square plate

h/a	*w* (1)	M_x (2)	M_y (2)
0.01	0.4066	4.7902	4.7902
0.05	0.4114	4.7902	4.7902
0.10	0.4271	4.7902	4.7902
0.2	0.4899	4.7902	4.7902

(1) $qa^4/1000D$; (2) $qa^2/100$

Table 3 Bending analysis of a CSCS rectangular plate ($h/a = 0.1$)

a/b	SSSS		
	w (1)	M_x (2)	M_y (2)
0.5	8.868	8.773	11.417
1.0	2.203	2.568	3.324
2.0	0.252	0.3702	1.058

(1) $qa^4/1000D$; (2) $qa^2/100$

Table 4 Numerical results for a CCCC trapezoidal plate ($a/b = 1.0$; $c/a = 0.7$)

h/a	*w* (1)	M_x (2)	Q_y (3)
0.01	0.00857	0.02088	0.7745
0.05	0.00937	0.02090	0.7886
0.10	0.01046	0.02092	0.7918
0.15	0.01279	0.02101	0.8111
0.2	0.01603	0.02104	0.8353

(1) $qa^4/1000D$; (2) $qa^2/100$; (3) $qa/100$

concentrated load are listed in Table 7 for two different boundary conditions. Also four different skew angles are taken into consideration. The results given by Butalia *et al*. (1990) have also given in this

table for comparisons. Butalia *et al*. (1990) presented a nine-node heterosis element based on finite element method (FEM) for skew rhombic plate. The present results are also agreed well with those values computed by FEM. Non-dimensional axial stress ($\sigma_x h^2/qa^2$) at the top surface and the non-dimensional central deflection of square plate for different side-to-thickness ratio is shown in Figs. 7 to 8. It is shown in these figures that the axial stress and deflections always increases with increasing side-to-thickness ratio. It is also concluded that, boundary conditions are significant on stress and deflections. Namely, the axial stress and deflections of SSSS plate are bigger than CCCC plate.

Fig. 9 shows a comparison study of the present DSC results with converged finite element (FE) solutions calculated by SAP 2000 software package. In this example the following values are

Table 5 Central deflection and maximum moment of a skew plate ($h/a = 0.01$)

Boundary Conditions	Skew angle	w (1)	M_x (2)
CCCC	30°	0.01702	0.25026
	45 °	0.06048	0.29113
	60 °	0.12347	0.31581
SSSS	30°	0.06511	0.06842
	45 °	0.21425	0.01256
	60 °	0.41034	0.01688

(1) $qa^4/1000D$; (2) $qa^2/100$

Table 6 Central deflection and bending moments of a SSSS skew plate

h/a	Skew angle	w (1)	M_c (max) (2)
0.05	15 °	0.00733	0.02595
	30°	0.06938	0.07802
	45 °	0.21802	0.13004
	60 °	0.41719	0.17068
	90 °	0.65904	0.19233
0.10	15 °	0.00971	0.02614
	30°	0.07736	0.07817
	45 °	0.23208	0.13106
	60 °	0.43722	0.17163
	90 °	0.68372	0.19202
0.15	15 °	0.01383	0.02619
	30°	0.09061	0.07806
	45 °	0.25582	0.13710
	60 °	0.47064	0.17101
	90 °	0.73009	0.19168
0.20	15 °	0.01943	0.02632
	30°	0.10997	0.07826
	45 °	0.29016	0.13115
	60 °	0.51803	0.17084
	90 °	0.78515	0.20053

(1) $qa^4/1000D$; (2) $qa^2/100$

Table 7 Maximum deflection of a skew plate under central concentrated load

Boundary Conditions	Skew angle	w_{max} (1)	
		Present DSC results	FEM results Butalia *et al.* (1990)
CCCC	30°	0.05703	0.05635
	45°	0.12004	0.11481
	60°	0.17105	0.17030
	75°	0.21056	0.20955
SSSS	30°	0.10934	0.10729
	45°	0.24001	0.23088
	60°	0.35981	0.35216
	75°	0.43955	0.43524

(1) $Pa^2/1000D$

considered: $h = 8$ cm; $a = b = 800$ cm; $\nu = 0.3$; E = 8736 kN/cm^2; $q = 16$ kN/m. When N=24 the FE result is converged whereas, the present DSC results are not changed with grid numbers for N>16. Namely, a reasonable accurate results are obtained for $N = 16$ in DSC method. A good agreement is achieved between the present results and FE solutions for $N = 24$.

As the last example a simply supported highly skewed rhombic plate (Morley's plate) subject to uniformly distributed load for skew angles 30°. The central deflections are obtained. A comparison solution of 0.408 has been obtained by Morley (1963) for $h/a = 0.01$. Results are shown in Fig.10 for two different side-to-thickness ratios. It is shown that the accuracy of the proposed method is suitable when using 15 grid points. For Morley's plate ($h/a = 0.01$) the accurate results are obtained as 0.409 for $N = 15$.

7. Concluding remarks

The method of discrete singular convolution for the static analysis of Mindlin-Reissner plates has

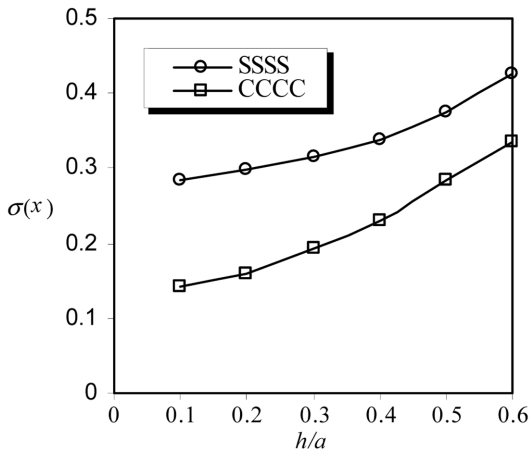

Fig. 7 Non-dimensional axial stress at the top surface of square plate for different side-to-thickness ratio

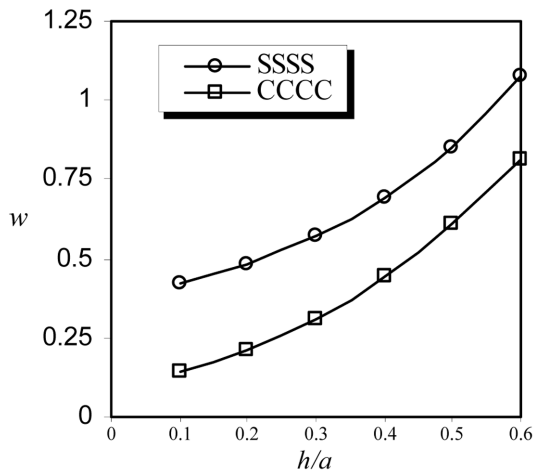

Fig. 8 Non-dimensional central deflection of square plate for different side-to-thickness ratio

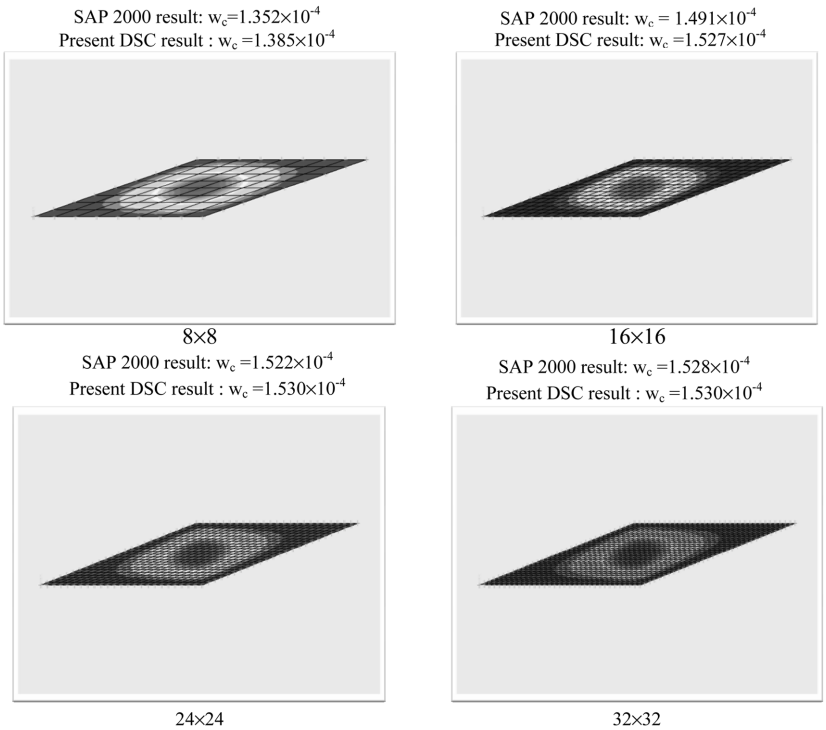

Fig. 9 Comparisons of SAP2000 and present DSC results of central displacement of CCCC skew plates for different grid numbers ($\alpha = 15^o$)

been presented for the first time. In the proposed approach, irregular physical domain is transformed into a rectangular domain by using the geometric coordinate transformation. The DSC procedures are then applied to discrete the transformed set of governing equations and boundary conditions. Numerical

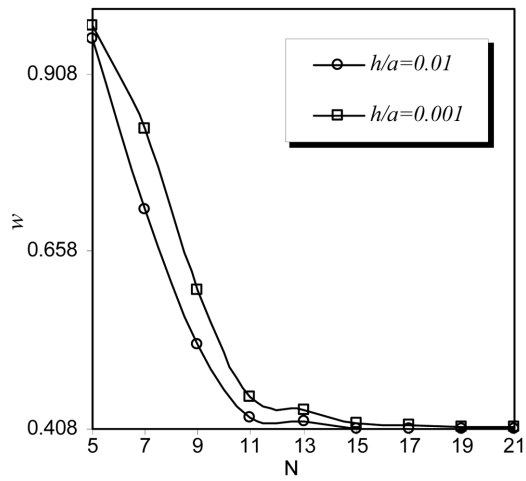

Fig. 10 Convergence of rhombic plates

results for the bending analysis are discussed. It is appeared that the grid numbers N and kernel parameter r of the singular convolution have been found to have a significant influence on the numerical results. The thickness to side ratio, h/a has also been found to have significant influence on the bending and deflection response of the skew plate. Furthermore, the decreasing value of the skew angle always decreases the convergence rate for the results of deflection. The proposed method is validated by comparing the present results with the analytical and numerical solutions available in the literature. Even though the analysis presented is for the straight-sided quadrilateral domain case only, the Reissner-Mindlin plates with curvilinear quadrilateral planforms also can be analyzed using the eight-node quadrilateral domain and is presently under study.

Acknowledgements

The financial support of the Scientific Research Projects Unit of Akdeniz University is gratefully acknowledged.

References

Ayad, R. and Rigolot, A. (2002), "An improved four-node hybrid-mixed element based upon Mindlin's plate theory", *Int. J. Number. Meth. Eng.*, **55**, 705-731.

Butalia, T.S., Kant, T. and Dixit, V.D. (1990), "Performance of heterosis element for bending of skew rhombic plates", *Comput. Struct.*, **34**(1), 23-49.

Cheung, Y.K., Tham, L.G. and Li, W.Y. (1988), "Free vibration and static analysis of general plates by spline finite strip method", *Comput. Mech.*, **3**, 187-197.

Civalek, Ö. (2004), "Application of Differential Quadrature (DQ) and Harmonic Differential Quadrature (HDQ) For Buckling Analysis of Thin Isotropic Plates and Elastic Columns", *Eng. Struct.*, **26**(2), 171-186.

Civalek, Ö. (2006), "An efficient method for free vibration analysis of rotating truncated conical shells", *Int. J. Pres. Ves. Pip.*, **83**, 1-12.

Civalek, Ö. (2006a), "Free vibration analysis of composite conical shells using the discrete singular convolution algorithm", *Steel Compos. Struct.*, **6**(4), 353-366.
Civalek, Ö. (2007), "Numerical analysis of free vibrations of laminated composite conical and cylindrical shells: discrete singular convolution (DSC) approach", *J. Comput. Appl. Math.*, **205**, 251- 271.
Civalek, Ö. (2007a), "Nonlinear analysis of thin rectangular plates on Winkler-Pasternak elastic foundations by DSC-HDQ methods", *Appl. Math. Model.*, **31**, 606-624.
Civalek, Ö. (2007b), "Three-dimensional vibration, buckling and bending analyses of thick rectangular plates based on discrete singular convolution method", *Int. J. Mech. Sci.*, **49**, 752-765.
Han, J.B., Liew, K.M. (1997), "An eight-node curvilinear differential quadrature formulation for Reissner/ Mindlin plates", *Comput. Methods Appl. M.*, **141**, 265-280.
Hou, Y., Wei, G.W. and Xiang, Y. (2005), "DSC-Ritz method for the free vibration analysis of Mindlin plates", *Int. J. Number. Meth. Eng.*, **62**, 262-288.
Kirchhoff, G. (1850), "Uber das gleichewicht und die bewegung einer elastischen scheibe", *J. Reine Angew. Math.*, (Crelle) **40**, 51.
Li, W.Y., Cheung, Y.K. and Tham, L.G. (1986), "Spline finite strip analysis of general plates", *J. Eng. Mech., ASCE*, **112**(1), 43-54.
Liew, K.M. and Han, J.B. (1995), "Bending analysis of simply supported shear deformable skew plates", *J. Eng. Mech., ASCE*, **123**(3), 214-221.
Liew, K.M., Xiang, Y., Kitipornchai, S. and Lim, M.K. (1994), "Vibration of Mindlin plates on point supports using constraint functions", *J. Eng. Mech.*, *ASCE*, **120**,499-513.
Liew, K.M., Xiang, Y., Kitipornchai, S. (1996), "Analytical buckling solutions for Mindlin plates involving free edges", *Int. J. Mech. Sci.*, **38**(10), 1127-1138.
Liew, K.M., Liu, F.L. (2000), "Differential quadrature method for vibration analysis of shear deformable annular sector plates", *J. Sound Vib*., **230**(2), 335-356.
Liew, K.M. and Han, J.B. (1997), "A four–note differential quadrature method for straight-sided quadrilateral Reissner/Mindlin plates", *Commun. Numer. Meth. En.*, **13**, 73-81.
Liu, F.L. and Liew, K.M. (1998), "Differential cubature method for static solutions of arbitrarily shaped thick plates", *Int. J. Solids Struct*., **35**(28-29), 3655-3674.
Liu, F.L., Liew, K.M. (1999), "Free vibration analysis of Mindlin sector plates: numerical solutions by differential quadrature method", *Comput. Methods Appl. M.*, **177**, 77-92.
Mindlin, R.D. (1951), "Influence of rotary inertia and shear on flexural motion of isotropic elastic plates", *J. Appl. Mech.*, *ASME*, **18**, 31-38.
Morley, L.S.D. (1963), *Skew plates and structures*, The Macmillan Company, New York.
Reissner, E. (1945), "The effect of transverse shear deformation on the bending of elastic plates", *J. Appl. Mech., ASME*, **12**, 69-77.
Timoshenko, S.P. and Woinowsky Krieger, S. (1959), *Theory of plates and shells*, McGraw-Hill, New York.
Wanji, C. and Cheung, Y.K. (2000), "Refined quadrilateral element based on Mindlin/Reissner plate theory", *Int. J. Numer. Meth. Eng*., **47**, 605-627.
Wang, C.M., Kitipornchai, S., Xiang, Y. and Liew, K.M. (1993), "Stability of Skew Mindlin Plates under Isotropic In-Plane Pressure", *J. Eng. Mech.*, *ASCE*, **119**, 393-401.
Wei, G.W. (2000), "Wavelets generated by using discrete singular convolution kernels", *J. Phys. A: Math. Gen.*, **33**, 8577-8596.
Wei, G.W. (2001), "A new algorithm for solving some mechanical problems", *Comput. Meth. Appl. M.*, **190**, 2017-2030.
Wei, G.W. (2001a), "Vibration analysis by discrete singular convolution", *J. Sound Vib*., **244**, 535-553.
Wei, G.W. (2001b), "Discrete singular convolution for beam analysis", *Eng. Struct.,* **23**, 1045-1053.
Wie, G.W., Zhao, Y.B. and Xiang, Y. (2002), "Discrete singular convolution and its application to the analysis of plates with internal supports, Part 1: Theory and algorithm", *Int. J. Numer. Meth. Eng*., **55**, 913-946.
Wei, G.W., Zhao, Y.B. and Xiang, Y. (2002a), "A novel approach for the analysis of high-frequency vibrations", *J. Sound Vib*., **257**(2), 207-246.
Xiang, Y. (2003), "Vibration of circular Mindlin plates with concentric elastic ring supports", *Int. J. Mech. Sci.,* **45**(3), 497-517.

Xiang, Y. and Wei, G.W. (2004), "Exact solutions for buckling and vibration of stepped rectangular Mindlin plates", *Int. J. Solids Struct*., **41**(1), 279-294.

Xiang, Y. and Zhang, L. (2005), "Free vibration analysis of stepped circular Mindlin plates", *J. Sound Vib*., **280**(3-5) 633-655.

Zhao, Y.B., Wei, G.W. and Xiang, Y. (2002), "Discrete singular convolution for the prediction of high frequency vibration of plates", *Int. J. Solids Struct*., **39**, 65-88.

Zhao, Y.B., Wei, G.W. and Xiang, Y. (2002a), "Plate vibration under irregular internal supports", *Int. J. Solids Struct*., **39**, 1361-1383.

CC